PERGAMON

Scripta Materialia 45 (2001) 33–40

Scripta MATERIALIA

www.elsevier.com/locate/scriptamat

Shear and tensile pseudoelastic behaviours of CuZnAl single crystals

A. Vivet[ab*], L. Orgéas[c], C. Lexcellent[a], D. Favier[c], and J. Bernardini[d]

[a] *Laboratoire de Mécanique Appliquée R. Chaléat-UMR CNRS 6604, Université de Franche-Comté – Institut des Microtechniques de Franche-Comté FR 0067, 25000 Besançon, France*

[b] *Laboratoire Universitaire de Recherche Scientifique d'Alençon, Université de Caen Basse-Normandie-IUT d'Alençon, 61250 Damigny, France*

[c] *Laboratoire Sols, Solides et Structures-UMR CNRS 5521, Université Joseph Fourier – Institut National de Polytechnique de Grenoble, B.P. 53, 38041 Grenoble Cedex 9, France*

[d] *Laboratoire de métallurgie-UMR CNRS 6518, Université d'Aix-Marseille III, 13397 Marseille Cedex 13, France*

Received 16 December 2000; accepted 1 March 2001

Keywords: Mechanical properties; Phase transformations; Shape memory alloys; Single crystal

Introduction

Shape memory alloys (SMA) are attractive materials as sensors or actuators for some adaptive structures. Improving the design of these smart SMA structures requires a better understanding of the basic and intrinsic mechanisms of thermoelastic stress-induced martensitic transformation. To that end, the study of the thermomechanical behaviour of SMA single crystals appears to be an appropriate solution, making it possible to avoid extrinsic effects induced by grain boundaries and other defects inherent to polycrystalline samples. Being easily and quickly performed, uniaxial tensile testing has been widely used to analyse the pseudoelastic behaviour of SMA single crystals [1,2]. However, combined with other kinds of mechanical loading, such as simple shear, tensile experiments would obviously bring a better knowledge of stress-induced martensitic transformation in SMA. For that purpose, CuZnAl single crystals were elaborated and deformed at temperatures above A_f using tensile and simple shear deformation modes. To the author's knowledge, the shear tests presented in this paper are the first to have been performed on SMA single crystals. They are compared with more classical tensile tests whose results have been previously published [3,4].

* Corresponding author. Address: Laboratoire Universitaire de Recherche Scientifique d'Alençon, Université de Caen Basse-Normandie-IUT d'Alençon, 61250 Damigny, France.

E-mail address: avivet@iutalencon.unicaen.fr (A. Vivet).

PII: S1359-6462(01)00988-5

Conclusions deduced from experiments will be useful to validate the basic assumptions of micro-mechanical models [3–5].

Experimental procedure

Starting from an industrial ingot provided by the company Tréfimétaux (Cu–25.63 Zn–4.2 Al wt.%), two single crystals (i.e. one for shear experiments and one for tensile experiments) were grown in a vertical furnace by the Bridgman method using a graphite crucible sealed in a quartz capsule under a pure 6N argon atmosphere. Briefly, as discussed in Ref. [3], the crucible was heated up to 1323 K, maintained for 60 min at this temperature. Therewith, the furnace was moved upwards at an optimised rate of 1 mm/min to reach the "betatisation" temperature (1123 K). The samples remained at this temperature for 25 min before breaking the quartz capsule by gravity in warm water (333 K). In order to minimise internal stresses, samples were finally aged in a quenching bath for 30 min at 333K.

Temperatures, at stress free state, of forward (austenite A $\rightarrow$ martensite M) and reverse (M $\rightarrow$ A) phase transitions of the shear specimen were determined by electrical resistivity measurements in a silicone oil bath. These characteristic temperatures are summarised in Table 1.

Crystallographic parameters of single crystals were also determined, noting $\Omega(\mathbf{x}_1, \mathbf{x}_2, \mathbf{x}_3)$ the geometrical reference of the sample and $\Omega'(\mathbf{x}'_1, \mathbf{x}'_2, \mathbf{x}'_3)$ the crystallographic reference of austenite unit cell. The loading axis for both shear and tensile samples, i.e. $\mathbf{x}_3$, is parallel to the major length of the samples. The crystallographic orientation of Ω towards Ω' was determined by back reflection Laüe method. Table 2 gives the orientation of axis $\mathbf{x}_3$ in the crystallographic reference frame Ω' both for the tensile and the shear single crystals. The austenite phase β_3 has a L21 structure with a cubic unit cell; while the martensite phase β'_3 presents a monoclinic structure with a M18R stacking arrangement: lattice parameters of Cu25.63Zn4.2Al wt.% single crystals were determined using X-ray technique, as listed in Table 3. With the help of these parameters and the phenomenological theory of martensite crystallography, named

Table 1
Characteristic values of thermal forward and reverse transformation

M_f (K)	M_s (K)	A_s (K)	A_f (K)
288.5	292.3	293.2	298.3

Table 2
Orientation of the loading axis $\mathbf{x}_3$ in the crystallographic reference of austenite unit cell Ω'

Sample	Axis $\mathbf{x}_3$ in Ω'		
Tensile	0.640	−0.022	0.742
Shear	−0.616	−0.588	0.515

Table 3
Lattice parameters of the Cu–25.63Zn–4.2Al wt.% single crystals from C. Satto (EMAT University of Antwerp)

a_{β_3}	$a_{\beta'_3}$	$b_{\beta'_3}$	$c_{\beta'_3}$	θ
5.870 Å	4.441 Å	5.530 Å	38.13 Å	89.08°

WLR [6,7], the habit plane normal **n**, the shearing direction **e** along the habit plane and the intrinsic shear strain g (=0.184) associated with the phase austenite to martensite transition were determined. The 24 possible variants of martensite, listed in Table 4, were then obtained by loop permutation of **n** and **e** vector direction cosines.

Isothermal monotonic tensile tests were carried out on an Instron 6025 universal testing machine equipped with an air furnace [3]. To perform these tests, a cylindrical single crystal (25 mm gauge length and 4 mm diameter) was used. The testing temperature was measured using a thermocouple placed in a sample head. Isothermal centred cyclic shear tests were performed on a single crystal sheet ($2 \times 10 \times 25$ mm^3, gauge volume $2 \times 3 \times 25$ mm^3) using a specific testing apparatus mounted on an Adamel-MTS DY35 universal testing machine [8,9]. The testing temperature was achieved

Table 4
Unit vectors **n** normal to the habit planes and unit vectors **e** along the displacement directions in the crystallographic reference Ω' – Orientation factors for shear test (R_{32}) and tensile test (R_{33}) in references Ω of the shear and tensile samples

Variant	n_1	n_2	n_3	e_1	e_2	e_3	R_{32}	R_{33}
1	−0.189	0.691	0.698	−0.172	−0.754	0.634	−0.021	−0.255
2	−0.189	0.698	0.691	−0.172	0.634	−0.754	0.061	0.140
3	0.189	0.691	0.698	0.172	−0.754	0.634	−0.038	−0.286
4	0.189	0.698	0.691	0.172	0.634	−0.754	0.053	0.379
5	−0.691	−0.189	0.698	0.754	−0.172	0.634	−0.457	−0.225
6	−0.698	−0.189	0.691	−0.634	−0.172	−0.754	0.363	0.334
7	−0.691	0.189	0.698	0.754	0.172	0.634	−0.339	−0.209
8	−0.698	0.189	0.691	−0.634	0.172	−0.754	0.361	0.096
9	−0.189	−0.691	0.698	−0.172	0.754	0.634	0.024	−0.281
10	−0.189	−0.698	0.691	−0.172	−0.634	−0.754	0.095	0.375
11	0.189	−0.691	0.698	0.172	0.754	0.634	−0.005	−0.265
12	0.189	−0.698	0.691	0.172	−0.634	−0.754	0.106	0.138
13	0.698	−0.189	0.691	0.634	−0.172	−0.754	0.380	0.098
14	0.691	−0.189	0.698	−0.754	−0.172	0.634	−0.451	−0.199
15	0.698	0.189	0.691	0.634	0.172	−0.754	0.358	0.337
16	0.691	0.189	0.698	−0.754	0.172	0.634	−0.332	−0.230
17	0.691	−0.698	0.189	−0.754	−0.634	0.172	−0.419	0.058
18	0.698	−0.691	0.189	0.634	0.754	0.172	0.311	−0.048
19	−0.691	0.698	0.189	0.754	0.634	0.172	−0.302	0.049
20	−0.698	0.691	0.189	−0.634	−0.754	0.172	0.318	−0.040
21	−0.698	−0.691	0.189	−0.634	0.754	0.172	0.333	−0.129
22	−0.691	−0.698	0.189	0.754	−0.634	0.172	−0.417	−0.031
23	0.698	0.691	0.189	0.634	−0.754	0.172	0.303	−0.135
24	0.691	0.698	0.189	−0.754	0.634	0.172	−0.296	−0.038

with a thermostatic oil bath (accuracy: ±0.1 K) and was controlled using a thermocouple fixed near the sample surface.

To reduce hysteretic effects induced by heat release and heat absorption associated with forward and reverse martensitic transformations [1,3], a very low tensile stress rate of 10^{-1} MPa s^{-1} and a very low shear strain rate of 1.7×10^{-3} s^{-1} were adopted for tensile and simple shear experiments, respectively. In order to stabilise the pseudoelastic behaviour [10], the shear sample was first submitted to a set of 50 centred cycles at 343 K under a magnitude shear strain of ±0.2. Similarly, a set of 10 loading–unloading cycles under a magnitude of 0.07 was applied to the tensile specimen. At last, to minimise creation and reorientation of self-accommodated martensite and to focus exclusively on the pseudoelastic behaviour, the mechanical tests were performed at temperatures higher than A_f i.e. 349 K for the tensile single crystal, and 323, 333, 343, and 353 K for the shear single crystal.

Results

In the (tensile stress–tensile strain) graph of Fig. 1 is plotted a full tensile pseudoelastic loop performed at 349 K, showing clearly the usual different steps of SMA pseudoelastic behaviour. Firstly, the loading curve is characterised by an initial stiff part along with the elastic austenite deformation as the main activated mechanism. The direct transition from austenite to martensite becomes the principal deformation mode after reaching a threshold tensile stress σ_{tr} (≈138 MPa) defined in Fig. 1: a strong decrease in the slope of the stress–strain curves is observed during a strain span cor-

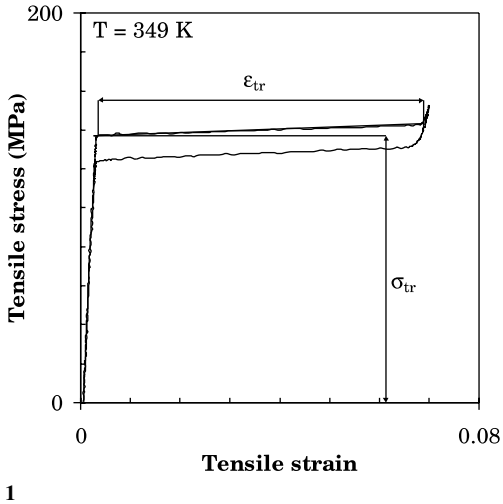

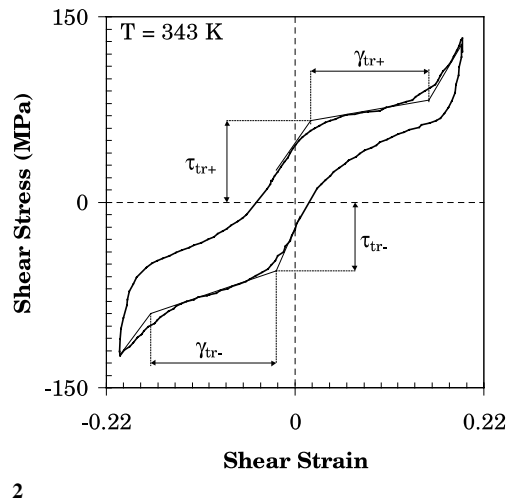

Fig. 1. Complete tensile pseudoelastic loop (349 K).
Fig. 2. Complete centred shear pseudoelastic loop (343 K).

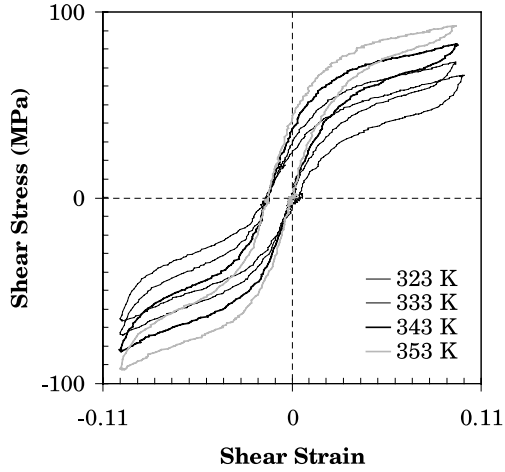

Fig. 3. Partial centred shear pseudoelastic loops (323, 333, 343 and 353 K).

responding to the conventional tensile transformation strain ε_{tr} ($\approx$0.066). Afterwards, the slope of the curve increases abruptly, showing that a major part of the gauge length is transformed. Decreasing the loading from this state leads to the reversion of the above phenomena, the reversion being characterised by a stress hysteresis.

In the (shear stress–shear strain) diagram of Fig. 2 is displayed a full centred shear pseudoelastic loop performed at 343 K under a shear strain span of $\pm$0.2. Compared to the tensile test of Fig. 1, a precise distinction between the different steps of the pseudoelastic behaviour is relatively more difficult to distinguish, as already mentioned in the case of shear pseudoelastic deformation of NiTi polycrystals [9,10]. Moreover, quite a large residual strain is observed at zero stress. Such a residual strain is supposedly induced by the presence of some partially stabilised martensite [10]. At last, based on conventional definitions quoted in Fig. 2, shear transformation stresses (i.e. τ_{tr+} when $\gamma > 0$ and τ_{tr-} when $\gamma < 0$) and strains (i.e. γ_{tr+} when $\gamma > 0$ and γ_{tr-} when $\gamma < 0$) were estimated, showing clearly that shear pseudoelastic deformation is asymmetric. As a matter of fact, τ_{tr+} equals $\approx$65 MPa while $|\tau_{tr-}|$ is only $\approx$53 MPa. Conversely, $|\gamma_{tr-}|$ ($\approx$0.152) is higher than γ_{tr+} ($\approx$0.134). Moreover, Fig. 2 also reveals that the hardening during stress-induced transformation, the stress hysteresis and the residual strain at zero stress are larger when $\gamma < 0$.

Fig. 3 displays a set of four shear pseudoelastic loops performed at different testing temperatures (323, 333, 343 and 353 K) under a shear strain span of $\pm$0.1. A well-known result is observed: the higher the testing temperature, the higher the stress level. Such a finding is further illustrated in Fig. 4, where transformation stresses τ_{tr+} and $|\tau_{tr-}|$, deduced from Fig. 3, have been plotted as functions of the testing temperature. In accordance with the Clausius–Clapeyron relation [11], a linear temperature evolution was found within the tested temperature range:

$$\tau_{tr+}\ (\mathrm{MPa}) = 1.035T\ (\mathrm{K}) - 289.7 \ \text{ and } \ |\tau_{tr-}|\ (\mathrm{MPa}) = 0.914T\ (\mathrm{K}) - 260.9$$

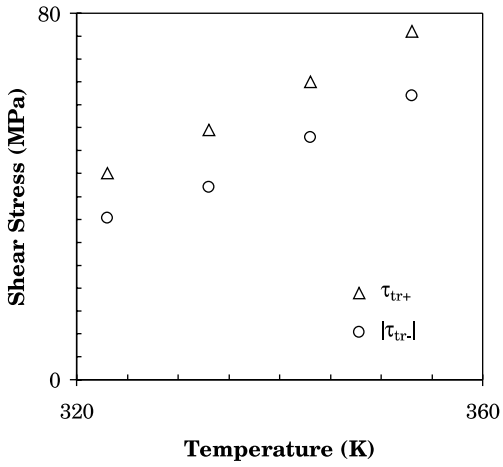

4

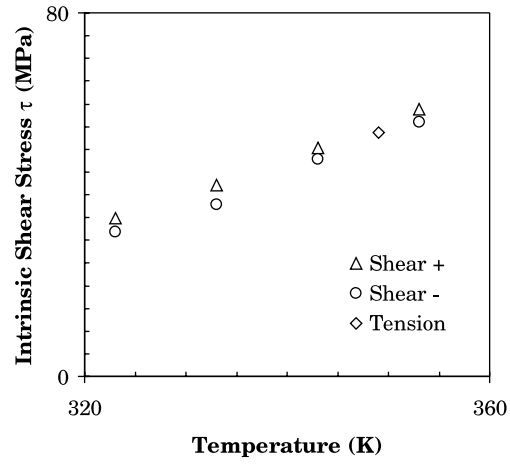

5

Fig. 4. Temperature evolution of transformation stresses according to Fig. 3.
Fig. 5. Temperature evolution of the estimated intrinsic transformation stress.

Discussion

Based on the WLR theory [6,7], it is assumed that for a given isothermal mechanical loading ($>A_f$), the first stress-induced martensite variant is, among the 24 possible variants, the one offering the greatest value R_{ij} of its orientation tensor **R** (i and j refer to the load axis).

$$\mathbf{R} = {}^{t}\mathbf{E}\mathbf{R}'\mathbf{E} \quad \text{with} \quad \left| \begin{array}{l} \mathbf{R}' = (1/2)(\mathbf{n} \otimes \mathbf{e} + \mathbf{e} \otimes \mathbf{n}) \text{ in the } \Omega' \text{ reference} \\ \mathbf{E} \text{ is the Euler rotation matrix defined by the orientation} \\ \quad \text{of } \mathbf{x}_3 \text{ in } \Omega' \end{array} \right.$$

As listed in Table 4, components R_{33} and R_{32} were determined for the tensile and simple shear samples, respectively. Assuming that the transformation strain associated with the first stress-induced martensite variant is the macroscopic experimental transformation strain determined during mechanical testing (i.e. ε_{tr} in tension, γ_{tr+} in shear "+", and γ_{tr-} in shear "−"), three experimental values of the intrinsic phase transformation strain g were determined:

$$g_{\text{tension exp}} = \varepsilon_{tr}/R_{33\ \max} \quad g_{\text{shear+exp}} = \gamma_{tr+}/2R_{32\ \max} \quad g_{\text{shear-exp}} = \gamma_{tr-}/2R_{32\ \min}$$

Results summarised in Table 5 first show that, due to the low crystallographic symmetry of martensite, the first stress-induced martensite variant predicted by the WLR theory is not the same in tension and compression, and not the same in shear "+" and shear "−". Asymmetric shear experimental results gained in the present work agree qualitatively with such predictions. Nevertheless, the intrinsic phase transformation strain deduced from shear and tensile experiments plotted in Figs. 1 and 2 are lower than the theoretical value ($g = 0.184$ with WLR theory). This discrepancy might be due

Table 5
Orientation factors R_{ij}, number of the activated variant calculated with WLR theory and intrinsic strain g deduced from experimental tests

Tensile	$\varepsilon > 0$			$\varepsilon < 0$		
	$R_{33\ max}$	Variant	$g_{tension\ exp}$	$R_{33\ min}$	Variant	$g_{com\ exp}$
	0.379	4	0.174	−0.286	3	–
Shear	$\gamma > 0$			$\gamma < 0$		
	$R_{32\ max}$	Variant	$g_{shear+exp}$	$R_{32\ min}$	Variant	$g_{shear-exp}$
	0.380	13	0.176	−0.457	5	0.166

to the appearance of other martensite variant(s) with smaller orientation factor during the deformation. This would lead to a minimisation of the experimental values of the intrinsic phase transformation strain given in Table 5. Such an assumption must be confirmed by some other experimental techniques during mechanical testing, like optical observations of the sample surface or diffraction measurements.

At last, an estimation of the intrinsic shear transformation stress τ associated with the first stress-induced variant was performed, based on all experimental data obtained in this work. τ was calculated using a simple transformation work criterion [12] and assuming that the transformation stress associated with the first stress-induced martensite variant is the macroscopic experimental transformation stress (i.e. σ_{tr} in tension, τ_{tr+} in shear "+", and τ_{tr-} in shear "−"):

$$\tau_{tension\ exp} = \sigma_{tr}\ R_{33\ max} \quad \tau_{shear+exp} = 2\tau_{tr+}R_{32\ max} \quad \tau_{shear-exp} = 2\tau_{tr-}R_{32\ min}$$

Results sketched in Fig. 5 show a fairly good correlation between tensile, shear "+" and shear "−" experiments. Moreover, a linear "Clausius–Clapeyron like" temperature evolution was found, in accordance with previous experimental results [1]:

$$\tau\ (\mathrm{MPa}) = 0.811T\ (\mathrm{K}) - 229.3$$

Conclusion

New mechanical tests on CuZnAl single crystals are presented. Despite the technological difficulties inherent to shear test setting, interesting results have been reached. The experimental conclusions can be summarised as follows:

(i) Due to the low crystallographic symmetry of martensite, the first stress-induced variant is a function of both the mechanical loading and the loading sense.
(ii) In the first stages of stress-induced martensitic transformation, a rather good accordance between experimental data and the WLR theory is found, i.e. the activation of a single variant of martensite among the 24 possible variants. However, other variant(s) may be stress induced during the last phase transition stages.

(iii) The main interest of shear test is emphasised, the possibility of studying two crystallographic directions on a specimen with only one mechanical test.

This paper presents the first step of more important experimental work, i.e. single crystal shear test development and validation. The second step is devoted to the study of the hysteresis occurring during pseudoelastic deformation of the single crystal. For that purpose, several complex loading paths have been carried out. The authors will present the results of these experiments in a future paper.

References

[1] Perin, P., Bourbon, G., Goo, B. C., Charai, A., Bernardini, J., & Lexcellent, C. (1995). J de Phys IV C2(5), 263.
[2] Patoor, E., Eberhardt, A., & Berveiller, M. (1987). Acta Metall 31(11), 2779.
[3] Lexcellent, C., Goo, B. C., Sun, Q. P., & Bernardini, J. (1996). Acta Mater 44(9), 3773.
[4] Goo, B. C., & Lexcellent, C. (1997). Acta Mater 45(2), 727.
[5] Vivet, A., & Lexcellent, C. (1998). Eur Phys J AP 24(2), 125.
[6] Wechsler, M. S., Lieberman, D. S., & Read, T. A. (1953). Trans AIME J Metals 197, 1503.
[7] Schroeder, T. A., & Wayman, C. M. (1979). Acta Mater 27, 405.
[8] Manach, P. Y., & Favier, D. (1997). Mat Sci Eng A 222, 45.
[9] Orgéas, L., & Favier, D. (1998). Acta Mater 46(15), 5579.
[10] Orgéas, L., Liu, Y., & Favier, D. (1997). J de Phys IV C5(7), 477.
[11] Wollants, P., De Bonte, M., & Roos, J. F. (1979). Z Metallkde 70, 113.
[12] Buchheit, T. E., & Wert, J. A. (1996). Met Trans A 27, 269.